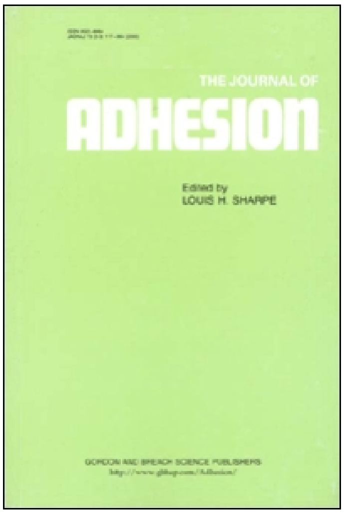

The Journal of Adhesion
Publication details, including instructions for authors and subscription information:
http://www.informaworld.com/smpp/title~content=t713453635

Elastic Analysis of the Loop Tack Test for Pressure Sensitive Adhesives

Raymond H. Plaut[a]; Nurocha L. Williams[a]; David A. Dillard[a]
[a] Center for Adhesive and Sealant Science, Virginia Polytechnic Institute and State University, Blacksburg, VA, USA

To cite this Article Plaut, Raymond H. , Williams, Nurocha L. and Dillard, David A.(2001) 'Elastic Analysis of the Loop Tack Test for Pressure Sensitive Adhesives', The Journal of Adhesion, 76: 1, 37 — 53
To link to this Article: DOI: 10.1080/00218460108029616
URL: http://dx.doi.org/10.1080/00218460108029616

J. Adhesion, 2001, Vol. 76, pp. 37–53
Reprints available directly from the publisher
Photocopying permitted by license only

Elastic Analysis of the Loop TackTest for Pressure Sensitive Adhesives

RAYMOND H. PLAUT*, NUROCHA L. WILLIAMS and DAVID A. DILLARD

Center for Adhesive and Sealant Science, Virginia Polytechnic Institute and State University, Blacksburg, VA 24061-0201, USA

(Received 31 August 2000; In final form 15 November 2000)

The behavior of pressure sensitive adhesive (PSA) tapes is sometimes examined *via* the loop tack test, in which a loop of the tape is brought into contact with a flat surface and then pulled away. A numerical analysis of the test is presented here. The loop is treated as an elastica, but with a nonlinear moment-curvature relation, so that the material is assumed to be elastic and inextensible. Debonding at the edge of the contact region is assumed to occur when the adhesive reaches a critical elongation. This elongation is assumed to depend on the maximum contact pressure and, in part of the results, on the length of time of contact. Shapes of the loop and values of the corresponding forces are obtained using a shooting method, and the effects of the stiffness and thickness of the adhesive and backing are examined.

Keywords: Loop tack; Pressure sensitive adhesive; Numerical analysis; Elastica; Elastic foundation; Shooting method

1. INTRODUCTION

The loop tack test has been used in industry to investigate the behavior of a strip (*e.g.*, a tape) consisting of a backing with a pressure sensitive adhesive. The ends of the highly-flexible strip are brought together and clamped, with the adhesive on the outside, to form a teardrop shape

*Corresponding author. Tel.: 540-231-6072, Fax: 540-231-7532, e-mail: rplaut@vt.edu

(see Fig. 1a). The top of the strip is moved downward and the loop makes contact with a horizontal, rigid substrate. After a certain contact area is attained, the loop may be held for a short time (the dwell time) and then the top is pulled upward until the loop separates from the substrate. Measurements are made of the deflection at the top of the loop and the associated applied vertical force. Often the maximum force reached as the loop is pulled off the substrate is called the tack or pull-off force. The objective of this paper is to formulate the basic loop tack test mathematically and develop a simple numerical solution procedure to compute the essential characteristics of the behavior of the loop. Such a methodology could prove useful in interpreting the results of these tests, which reportedly depend on several factors in addition to the adhesive used.

Short descriptions of the loop tack test are presented in Pizzi and Mittal [1] and Satas [2]. Muny [3] discussed various PSA tests, including loop tack, and Lin [4] obtained separation forces for loop tack tests on four surfaces. The relation between ultraviolet dose and loop tack was examined by Brockmann and Geiss [5]. Chuang *et al.* [6] compared the Avery Adhesive Test with the loop tack test. Roberts [7, 8] described FINAT test method number 9 for loop tack and compared results of tests carried out on three sets of tapes by 13 laboratories, and Tobing and Klein [9] listed experimental results for loop tack.

Hu *et al.* [10], Duncan and Lay [11], and Duncan *et al.* [12] presented numerical results obtained with the use of the finite element

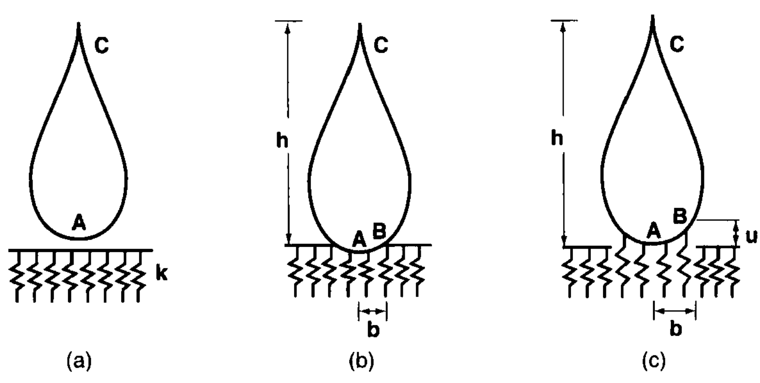

FIGURE 1 Illustration of (a) loop before contact with foundation, (b) pushing phase, and (c) pulling phase.

method. The loop was assumed to be elastic, and the tack force decreased as the stiffness or thickness of the backing increased. Plaut *et al.* [13, 14] examined the behavior of an elastica loop pressed against a rigid, flat surface. In [14], the work of adhesion between the loop and the substrate was modeled using JKR and DMT types of analyses.

Here the loop is an adhesive tape, consisting of a backing and a PSA. Various assumptions are made. The strip is unstrained when it is flat. It is thin, uniform, inextensible, and (unlike [13, 14]) nonlinearly elastic. Anticlastic curvature is neglected, as well as the weight of the strip. As the loop is pulled upward, it continuously debonds from the substrate at the ends of the contact zone when the adhesive reaches a certain critical elongation, which depends on the pressure that has been applied at that location and, in one part of this study, on the time of contact (but indirectly, since time dependence is not included in the analysis). The adhesive is assumed to be located on the substrate rather than on the loop, which is equivalent if the influence of the adhesive on the bending stiffness is neglected, and if the resisting forces only depend on the vertical elongation of the adhesive, as assumed here. (In fact, the adhesive is attached to the substrate in one of the standard British loop tack tests, and in the probe tack test [15].) The adhesive is modeled as an elastic Winkler foundation (*i.e.*, a continuous distribution of independent vertical springs), as has been done sometimes in the analysis of the peel test [16].

In the next section, the problem is formulated. Results for cases in which the contact time is not included are presented in Section 3. Equilibrium shapes and corresponding forces are determined. In Section 4, the contact time is introduced and results are obtained. Conclusions are given in Section 5.

2. FORMULATION

The "pushing" phase will refer to the period when the top of the loop is moving downward (Fig. 1b), and the "pulling" phase will refer to the subsequent time when the top is moving upward (Fig. 1c). The mathematical formulation and results will be presented in nondimensional terms. In Figure 1, point A represents the bottom of the loop, point B is at the right end of the contact zone, and point C is at the top of the loop. The height of point C above the unstrained level of the foundation is denoted h, and the distance of point B above that level is denoted u. Therefore $u = 0$ during pushing (when B is at the unstrained foundation level) and $u > 0$ during pulling (when the adhesive near the detachment point B is stretched). The horizontal distance b from A to B will be called the contact length.

Due to symmetry, only the right half of the loop will be analyzed, as shown in Figure 2a. For the section BC of the loop that is not in contact with the foundation, the horizontal coordinate is x, the vertical coordinate is y, the arc length is s, the total arc length from B to C is s_C, and the angle of the tangent with the horizontal is θ. At C, the horizontal and vertical forces are p and r, respectively, and the bending moment is m_C. For the section AB in contact with the foundation, the coordinates are ξ and η, the arc length is z, and the angle with the horizontal is ϕ. Both coordinate systems have their origin at B, to simplify the solution procedure. The bending moment at A is m_A and

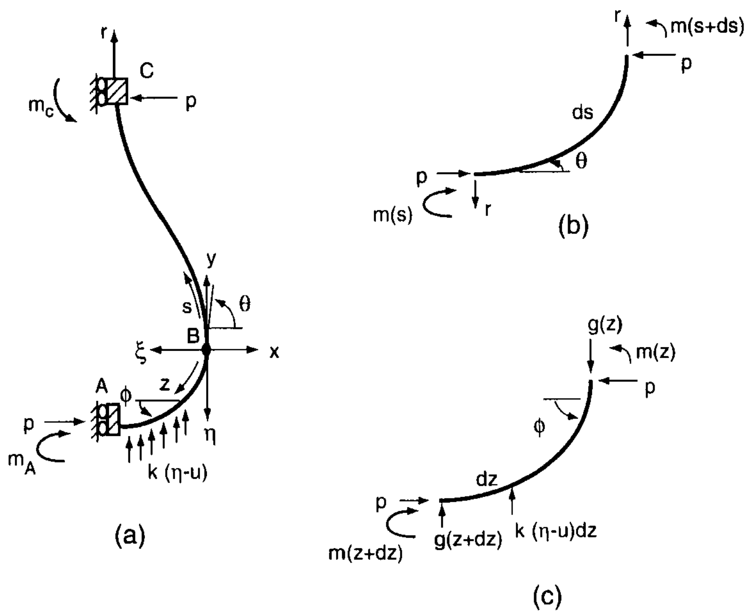

FIGURE 2 Illustration of (a) right half of loop, (b) free-body diagram of element in section BC, and (c) free-body diagram of element in section AB.

the horizontal force at A is p. Positive senses are shown in Figure 2a. The distributed force on section AB is $k(\eta - u)$ and acts upward if $\eta > u$.

The quantity r represents half the total vertical force on the loop at its top. Dimensional lengths can be obtained by multiplying the nondimensional lengths (such as h, u, b, x, and y) by L, which is half the dimensional length of the actual loop. Dimensional forces are found by multiplying nondimensional forces (such as p and r) by $EI/(L^2)$, where E is the initial modulus of elasticity of the backing and I is the moment of inertia of the rectangular cross section of the backing. Multiplying m, m_A, and m_C by EI/L furnishes dimensional bending moments. The nondimensional foundation stiffness, k, is related to the dimensional stiffness, K, of the adhesive by $k = KL^4/(EI)$.

In dimensional terms, if the backing and adhesive have width W, if the backing has thickness H_b, and if the adhesive has thickness H_a and is linearly elastic with modulus of elasticity E_a, then

$$K = \frac{E_a W}{H_a}, \tag{1a}$$

$$k = \frac{12 E_a L^4}{E H_a H_b^3}. \tag{1b}$$

For example, if $L = 45\,\text{mm}$, $E = 1{,}000\,\text{MPa}$, $E_a = 0.15\,\text{MPa}$, $H_b = 0.25\,\text{mm}$, and $H_a = 0.05\,\text{mm}$, then $k = 2.4 \times 10^6$. The stiffness, k, basically represents the relative stiffness of the adhesive to the backing. Numerical results will be presented for $k = 10^6$ and $k = 10^4$ (a stiffer backing).

The bending resistance of the adhesive is neglected. It is assumed that the moment-curvature relation for the backing follows a power law, with the material becoming weaker as it bends. The particular law chosen in the numerical examples will be given in Eqs. (2c) and (3c). It leads to maximum curvatures that are about twice as great as they would be for a linearly-elastic backing with modulus of elasticity E.

A free-body diagram of an element from s (at the bottom) to s+ds on segment BC is depicted in Figure 2b. The governing equations for segment BC are as follows:

$$\frac{dx}{ds} = \cos\theta, \tag{2a}$$

$$\frac{dy}{ds} = \sin\theta, \tag{2b}$$

$$\frac{d\theta}{ds} = m + 0.01\,m^3, \tag{2c}$$

$$\frac{dm}{ds} = -p\sin\theta - r\cos\theta. \tag{2d}$$

Equations (2a) and (2b) follow from geometry, Eq. (2c) is the nonlinear moment-curvature relation, and Eq. (2d) describes equilibrium of moments. Figure 2c shows a free-body diagram of an element from z (at the top) to z+dz on segment AB. The vertical force is g(z). The governing equations for segment AB, including equilibrium of vertical forces, are

$$\frac{d\xi}{dz} = \cos\phi, \tag{3a}$$

$$\frac{d\eta}{dz} = \sin\phi, \tag{3b}$$

$$\frac{d\phi}{dz} = -(m + 0.01\,m^3), \tag{3c}$$

$$\frac{dm}{dz} = p\sin\phi - g\cos\phi, \tag{3d}$$

$$\frac{dg}{dz} = -k(\eta - u). \tag{3e}$$

The boundary conditions at C are $x = -b$ and $\theta = \pi/2$. At A, $\xi = b$, $\phi = 0$, and $g = 0$ (due to symmetry of the loop). The conditions at B are as follows: x, y, ξ and η are zero, $\phi = \theta$, $g = -r$, and m is continuous.

Numerical solutions are obtained with the use of a shooting method [17]. The nondimensional length of the right half of the loop is unity. In order to combine Eqs. (2) and (3) with a single length, t, that varies from zero at B to unity at C and A, t is defined as s/s_C for Eqs. (2) and as $z/(1-s_C)$ for Eqs. (3). The nine equations are written in terms of t. There are seven "initial" conditions at $t=0$ (*i.e.*, at B), leaving two unknown initial conditions. The five unknown quantities are taken to be $\theta(0)$, m(0), r, p, and s_C. As described above, there are five known "end" conditions at $t=1$ (*i.e.*, at C and A). Thus, for fixed values of b, k, and u, the five unknown quantities are varied systematically until numerical integration of the nine governing equations from $t=0$ to $t=1$ leads to satisfaction of the five end conditions with sufficient accuracy. The programs NDSolve and FindRoot in Mathematica [18–20] are utilized to carry out this shooting procedure. Once the unknown quantities are computed, the forces, moments, and shape of the loop can be obtained.

3. DEBONDING INDEPENDENT OF CONTACT TIME

In this section, it is assumed that the debonding criterion depends on the pressure but not on the time of contact. The program is run for a series of values of the contact length, b. The loop is pushed down until $b=0.20$ (*i.e.*, the maximum contact length of the loop is one-fifth of the length of the loop), which is used in some loop tack tests. During the pushing phase, b is chosen to be 0.01, 0.02, ..., 0.20. The stiffness k is fixed, and $u=0$ in Eq. (3e). For each value of b, the numerical solution is obtained. With $k=10^6$, the shapes for contact lengths $b=0.01$, 0.05, 0.15, and 0.20 during pushing are shown in parts (a)–(d), respectively, of Figure 3.

Although it cannot be seen in Figure 3, the strip may oscillate in the contact region. Figure 4 uses a highly exaggerated scale of the nondimensional vertical deflection to show this for the whole contact region. When $b=0.05$, the deflection is not oscillatory, but when $b=0.10$, 0.15, and 0.20, the deflections have a local maximum at the center (point A) and then local minima before reaching zero deflection at the ends of the contact region (*i.e.*, at B). In fact, for $b=0.15$ and 0.20, the central part of the loop rises above the unstrained location of

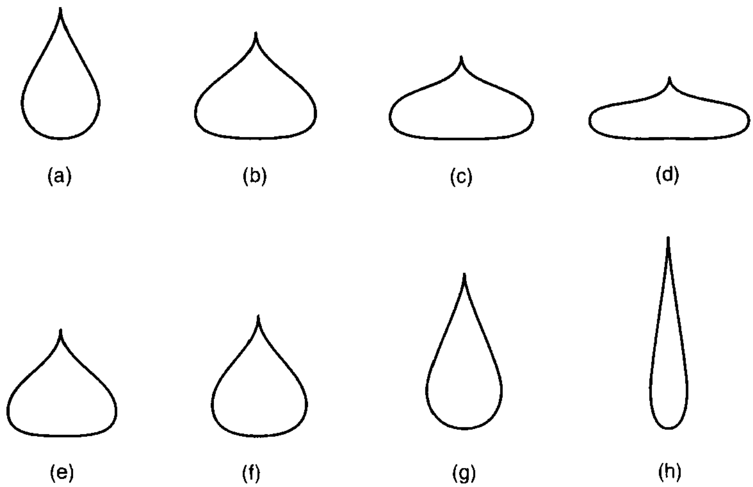

FIGURE 3 Equilibrium shapes of loop during pushing for $k=10^6$ with (a) $b=0.01$, (b) $b=0.10$, (c) $b=0.15$, and (d) $b=0.20$, and during pulling with (e) $b=0.15$, (f) $b=0.10$, (g) $b=0.05$, and (h) $b=0.015$.

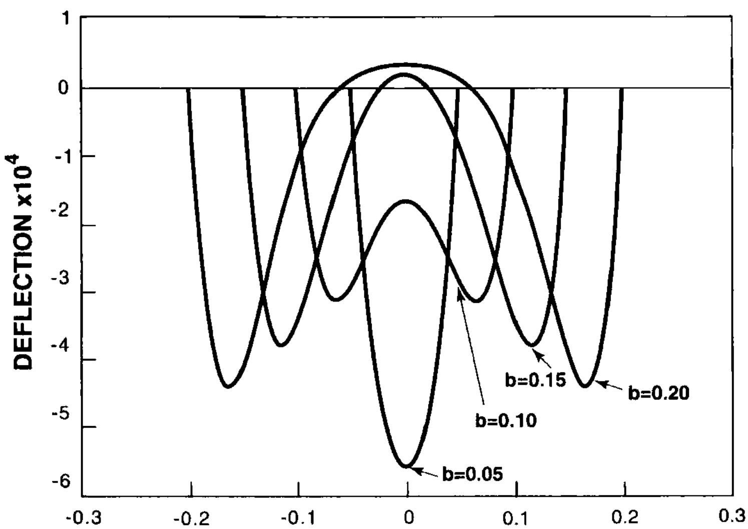

FIGURE 4 Illustration of deflection in contact region during pushing at four values of b for $k=10^6$.

the foundation and is pulled downward by the adhesive. These features also occur in problems involving beams attached to elastic foundations [21].

The bottom solid curve in Figure 5 shows how the vertical force, r, and the height, h, of point C are related. Just before the loop makes contact with the substrate, $h = 0.8486$, $p = 9.913$, $m_A = 5.384$, and $m_C = -3.028$ [13]. As the loop is pushed downward, r decreases to negative values and h decreases. At $b = 0.20$, it is found that $r = -30.2$, $h = 0.448$, $p = 4.14$, $m_B = 1.35$, $m_C = -6.55$, and $\theta_B = 0.030$, where m_B and θ_B denote the bending moment and angle (in radians), respectively, at point B. The relation for $k = 10^4$ is shown by the bottom solid curve in Figure 6. When $b = 0.20$ for this case, $r = -23.5$, $h = 0.581$, $p = 6.16$, $m_B = 2.95$, $m_C = -5.32$, and $\theta_B = 0.255$. Figures 7 and 8 show the corresponding relations between the force r and the contact length b along the bottom solid curves for $k = 10^6$ and $k = 10^4$, respectively. Naturally b increases as the top of the loop is pushed downward (*i.e.*, as r becomes more negative).

When the top of the loop is pulled upward, the adhesive resists debonding. The detachment point B lifts above the unstrained level of the foundation. It is assumed in this section that detachment occurs when the elongation of the foundation (*i.e.*, the adhesive) reaches the value $u = 5\eta_{max}$ where η_{max} is the maximum downward deflection that

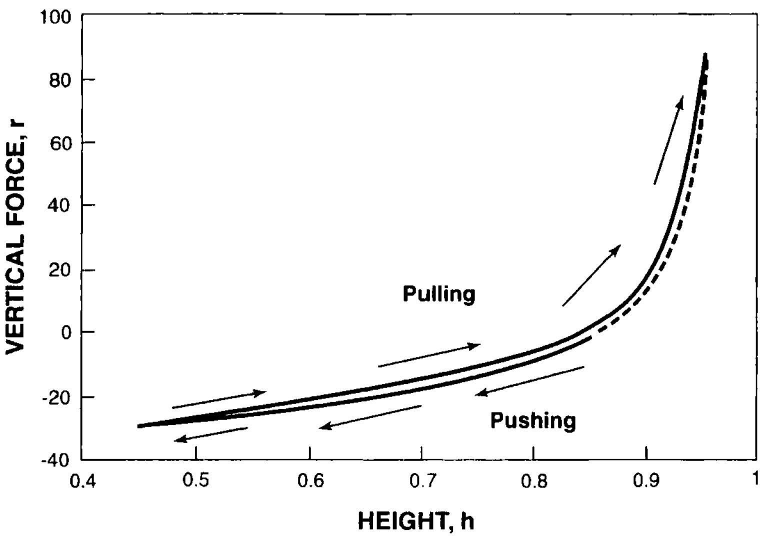

FIGURE 5 Vertical force *versus* loop height for $k = 10^6$.

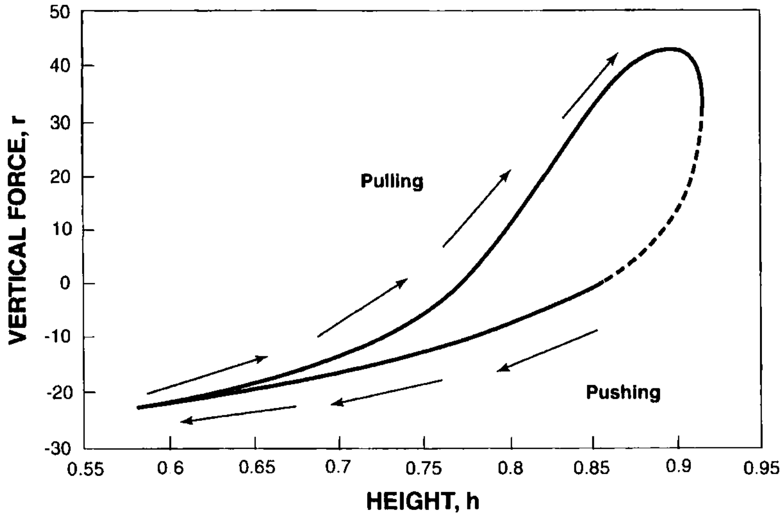

FIGURE 6 Vertical force *versus* loop height for $k = 10^4$.

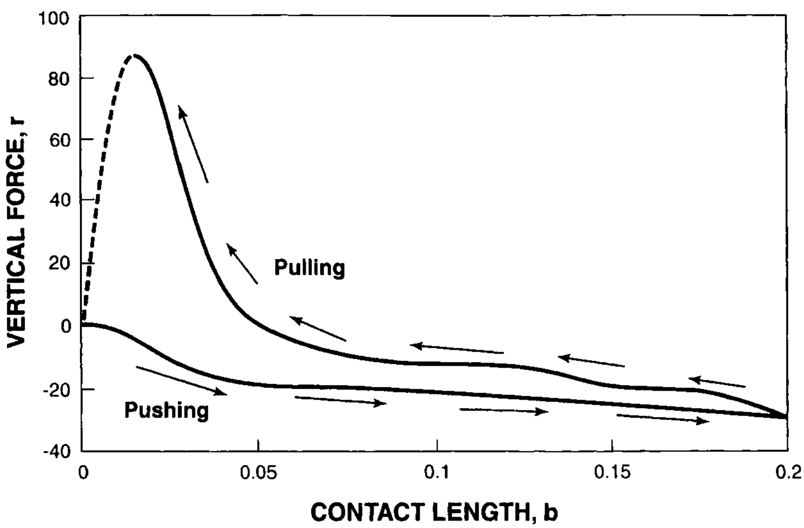

FIGURE 7 Vertical force *versus* contact length for $k = 10^6$.

occurred previously at that location. Since the foundation pressure is proportional to the deflection, this criterion is directly related to the maximum pressure. Creton [22], among others, stated that the tack of

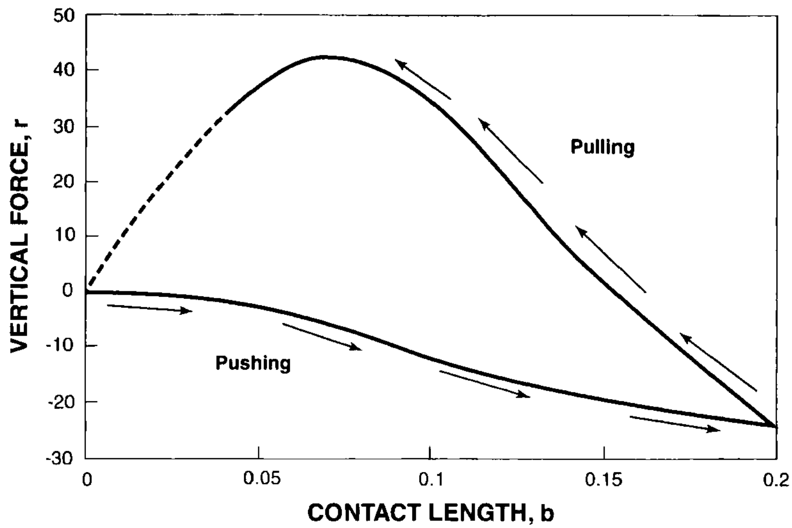

FIGURE 8 Vertical force *versus* contact length for $k = 10^4$.

PSAs increases with an increase in pressure. The factor five is chosen arbitrarily to obtain the numerical results in this study.

The maximum deflection that occurred is found numerically from the results at previously-considered values of contact length, b. First, b is set at 0.19. For $k = 10^6$, the downward deflection at that location at the end of pushing was 0.00024. Thus, the quantity u in Eq. (3e) is put equal to five times that value, and the system of equations is solved. Next, $b = 0.18$ is considered. At that location, the downward deflection when $b = 0.19$ during pushing was 0.00023, when $b = 0.20$ it was 0.00037, and when $b = 0.19$ during pulling the deflection was upward. Thus, u is taken as five times 0.00037 and the solution for $b = 0.18$ is obtained. This procedure is continued as pulling commences and b decreases, considering all previous deflection values. For $b = 0.15$ and smaller, the maximum downward deflection occurs during the previous part of the pulling phase rather than during the pushing phase, *i.e.*, the central part of the contact region is pushed further into the substrate as the top of the loop is pulled upward. When b becomes small, results are computed for additional values of b as the force and height increase toward their maximum values before pull-off takes place.

For $k = 10^6$ and 10^4, respectively, the upper solid curves in Figures 5 and 6 show the relation between r and h during pulling. Consider Figure 5 first. The initial part of this curve is only slightly above the curve for pushing. It then reaches a peak at $r = 88.9$, which is the nondimensional tack force. At this peak, $h = 0.956$, $b = 0.015$, $p = 13.2$, $m_B = 9.93$, $m_C = -1.39$, and $\theta_B = 0.329$. In the standard loop tack test, the displacement of the top of the loop is controlled and the curve continues a little further until h reaches its largest value, 0.957, and r reduces to 88.5. Separation of the loop from the substrate occurs at that point.

Dashed curves represent equilibrium states which exist mathematically between the point with the largest height, h, and the point at which the test cycle began. These states do not occur physically during the test, since the loop separates completely from the substrate before these states can be reached.

The scales in Figures 5 and 6 are not the same. For $k = 10^4$ in Figure 6, the tack force is $r = 43.1$. Associated quantities are $h = 0.899$, $b = 0.069$, $p = 11.9$, $m_B = 5.96$, $m_C = -1.76$, and $\theta_B = 0.829$. For displacement control, the largest value of h is 0.917, with a corresponding force $r = 32.6$. Due to a relatively stiffer backing here, these forces and heights are smaller than in Figure 5.

For $k = 10^6$, the shapes of the loop during pulling are depicted in parts (e)–(h) of Figure 3 for $b = 0.15$, 0.10, 0.05, and 0.015, respectively. Figure 9 shows the corresponding exaggerated shapes in

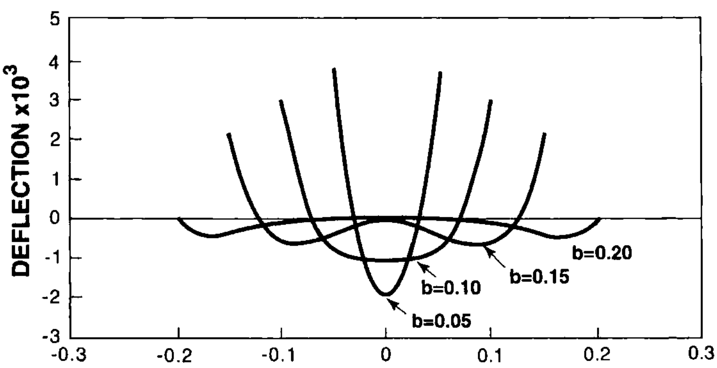

FIGURE 9 Illustration of deflection in contact region during pulling at four values of b for $k = 10^6$.

the contact region for $b = 0.20$. 0.15. 0.10, and 0.05. The plot for $b = 0.20$, at the end of pushing and beginning of pulling, naturally is the same as in Figure 4, but with a different vertical scale. In Figure 9, the values of the deflection, u, at the edge of the contact region are 0.0022, 0.0032, and 0.0039, respectively, for $b = 0.15$, 0.10, and 0.05. The shapes for the last two values of b do not oscillate.

4. INCLUSION OF CONTACT TIME

In standard loop tack tests, the top of the loop is pushed downward at a constant speed, and then pulled upward at the same constant speed. Sometimes there is no dwell time between these phases (*e.g.*, in FINAT test method number 9 [7]). If it assumed that the speed is constant and that the dwell time is negligible (or that the change of adhesion properties is negligible during the dwell time), then the effective time that a location on the strip is in contact with the substrate can be computed from the change of height during pushing and pulling.

Since the strip is almost flat in the contact region, a horizontal position is essentially associated with a location on the strip. For example, consider $b = 0.16$. Let h_I be the value of h when the loop initially comes into contact at $b = 0.16$ during pushing, let h_P be the height at the end of the pushing phase, and let h_D be the height when the loop detaches at $b = 0.16$. The total change is $\Delta h = (h_I - h_P) + (h_D - h_P)$. It is assumed in this section that the resistance to pull-off increases as the time of contact increases, so that the critical elongation length increases as Δh increases. To obtain numerical results, this length is arbitrarily chosen to be

$$u = (5 + 10\,\Delta h)\eta_{max}. \tag{4}$$

This criterion would be the same as in the previous section if the coefficient of Δh were set equal to zero. Since the value of h_D is not known until the solution is known (for the particular value of contact length, b), an iterative procedure is required.

Results for $k = 10^4$ are presented in Figures 10 (r *versus* h) and 11 (r *versus* b). Since the critical length of the adhesive for debonding is higher than in the previous section, the tack force will be higher.

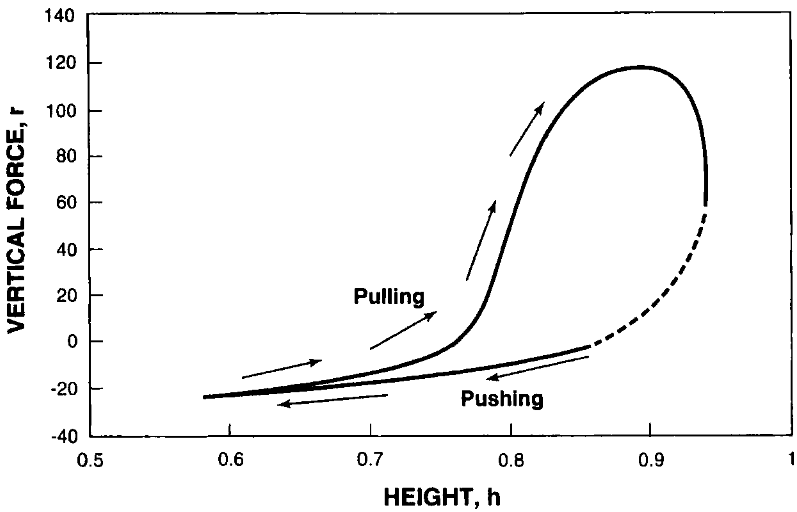

FIGURE 10 Vertical force *versus* loop height for $k = 10^4$ including effect of contact time.

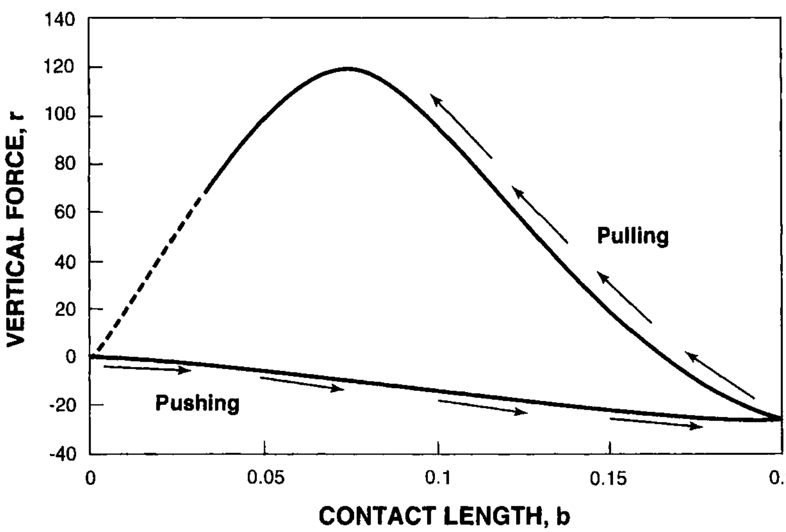

FIGURE 11 Vertical force *versus* contact length for $k = 10^4$ including effect of contact time.

Here it is $r = 118$ (compared with $r = 43.1$ in Figs. 6 and 8). Corresponding to this peak, $h = 0.905$, $b = 0.065$, $p = 16.2$, $m_B = 5.54$, $m_C = -1.48$, and $\theta_B = 1.15$. If the displacement is controlled, the loop separates when $h = 0.940$, where $r = 68.4$.

5. CONCLUDING REMARKS

A mathematical formulation of the loop tack test has been presented, and the governing equations were solved numerically with the use of a shooting method. Large deflections were considered. The adhesive tape was assumed to be nonlinearly elastic, with the bending resistance weakening as the moment increased. Stretching of the backing was neglected, as was its weight. The adhesive was modeled as being on the substrate, which is equivalent in this formulation to being attached to the backing. The adhesive was assumed to act as a distribution of independent, linearly-elastic springs, which detached from the loop after a critical elongation was attained.

The critical value for debonding was assumed to depend on the maximum pressure applied to the adhesive, and also in one case on the time of contact (assuming no dwell time exists between the pushing and pulling phases of the loop onto the substrate). Particular choices of the moment-curvature relation and the debonding criteria were made, but the formulation is applicable to other choices. The computer program Mathematica was applied to obtain numerical solutions in an approximate step-by-step procedure. Shapes of the loop during the cycle were determined, as well as values of forces. The maximum force required for separation of the loop from the substrate is the tack or pull-off force.

The shooting method transforms a boundary value problem into an initial value problem. Initial guesses are chosen for unknown parameters and initial conditions, and the differential equations are solved numerically. The method is accurate. For this highly nonlinear problem, however, convergence to the desired solution may be sensitive to the initial guesses. Sometimes the method converges to a mathematical solution which does not represent the actual physical loop. For a relative stiffness $k = 10^6$ and taking time of contact into account as in Section 4, the pulling force reached $r = 146$ [20] but further results were not obtained due to convergence difficulties and, hence, results for that case were not presented here.

The nondimensional stiffness, k, defined in Eq. (1b) is proportional to the ratio of the adhesive stiffness to the initial backing stiffness. It also depends on the thicknesses of the backing and adhesive, and on the length of the loop. The results indicate that the pull-off force increases as k increases, *i.e.*, as the stiffness of the backing or the thickness of the backing or adhesive decreases, or as the stiffness of the adhesive or the length of the loop increases.

The work presented here for an inextensible, nonlinearly-elastic loop represents an initial analysis of the loop tack test based on a set of governing differential equations. The results describe the main characteristics of the shapes and forces occurring during the test. This basic investigation is being extended to include other factors. Stretching of the loop during pulling may cause the curves to exhibit a plateau before separation occurs. Inelastic behavior of the loop may be important, especially during the final stages of the cycle. Viscoelastic behavior of the adhesive may have a significant effect. Various detachment criteria have been proposed for PSAs, including critical stress or strain, critical total stored elastic energy, and critical stored elastic energy density [23]. In conjunction with this analytical and numerical investigation, a set of experiments is underway to validate the theoretical models being developed.

Tack of a PSA tape depends on several factors, including the stiffness of the backing. There is a need to understand and interpret results obtained from loop tack tests. This paper is part of an investigation which will provide insights to those trying to utilize the results of such tests and to design PSA tapes.

Acknowledgements

This research was supported by the National Science Foundation under Grant No. CMS-9713949, and by a fellowship from the Adhesion and Sealant Council Education Foundation provided through the Center for Adhesive and Sealant Science at Virginia Tech. The authors are grateful to the reviewers for their helpful comments. They are also grateful to the Ashland Specialty Chemical

Company for providing discussions, funding, and materials to initiate a study in this area.

References

[1] Pizzi, A. and Mittal, K. L. Eds., *Handbook of Adhesive Technology* (Marcel Dekker, New York, 1994), pp. 98, 561.
[2] Satas, D. Ed., *Handbook of Pressure-Sensitive Adhesive Technology* (Van Nostrand Reinhold, New York, 1989), 2nd edn., p. 46.
[3] Muny, R. P., *Adhesives Age* **39**(9), 20 (1996).
[4] Lin, S. B., *J. Adhesion Sci. Technol.* **10**, 559 (1996).
[5] Brockmann, W. and Geiss, P. L., *Tappi J.* **80**, 167 (1997).
[6] Chuang, H. K., Chiu, C. and Paniagua, R., *Adhesives Age* **40**(10), 18 (1997).
[7] Roberts, R. A., *Report 5*, Project PAJ1, National Physical Laboratory, Teddington, United Kingdom (1997).
[8] Roberts, R. A., *Report 10*, Project PAJ1, National Physical Laboratory, Teddington, United Kingdom (1999).
[9] Tobing, S. D. and Klein, A., *J. Appl. Polym. Sci.* **76**, 1965 (2000).
[10] Hu, F., Olusanya, A., Lay, L. A., Urquhart, J. and Crocker, L., *Report 8*, Project PAJ1, National Physical Laboratory, Teddington, United Kingdom (1999).
[11] Duncan, B. C. and Lay, L. A., *Report 11*, Project PAJ1, National Physical Laboratory, Teddington, United Kingdom (1999).
[12] Duncan, B. C., Lay, L. A., Olusanya, A., Roberts, R. A. and Abbott, S. G., *Adhesion '99: Proc. Seventh Int. Conf. on Adhesion and Adhesives*, p. 313 (1999).
[13] Plaut, R. H., Suherman, S., Dillard, D. A., Williams, B. E. and Watson, L. T., *Int. J. Solids Structures* **36**, 1209 (1999).
[14] Plaut, R. H., Dalrymple, A. J. and Dillard, D. A., *J. Adhesion Sci. Technol.* (to be published).
[15] Duncan, B., Abbott, S. and Roberts, R., *Measurement Good Practice Guide No. 26*, National Physical Laboratory, Teddington, United Kingdom (1999).
[16] Kinloch, A. J., Lau, C. C. and Williams, J. G., *Int. J. Fract.* **66**, 45 (1994).
[17] Roberts, S. M. and Shipman, J. S., *Two-Point Boundary Value Problems: Shooting Methods* (Elsevier, New York, 1972).
[18] Wolfram, S., *Mathematica: A System for Doing Mathematics by Computer* (Addison-Wesley, Reading, Massachusetts, 1991).
[19] Bahder, T. B., *Mathematica for Scientists and Engineers* (Addison-Wesley, Reading, Massachusetts, 1995).
[20] Williams, N. L., *MS Thesis*, Virginia Polytechnic Institute and State University (2000).
[21] Hetenyi, M., *Beams on Elastic Foundation* (University of Michigan Press, Ann Arbor, Michigan, 1946).
[22] Creton, C., In: *Materials Science and Technology, Vol. 18: Processing of Polymers*, Cahn, R. W., Haasen, P. and Kramer, E. J. Eds. (Wiley-VCH, Weinheim, Germany, 1997), p. 707.
[23] Yarusso, D. J., *J. Adhesion* **70**, 299 (1999).